2015-05-25

# Health effects of selected nanoparticlesin vivo: liver function and hepatotoxicity following intravenous injection of titanium dioxide and Na-oleate-coated iron oxide nanoparticles in rodents

Volkovova, K



10.3109/17435390.2013.815285
Nanotoxicology
Informa UK Limited

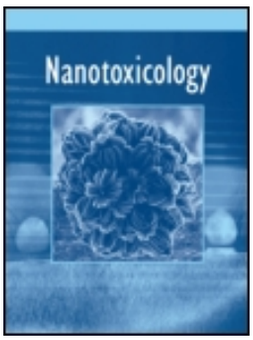

Nanotoxicology

ISSN: 1743-5390 (Print) 1743-5404 (Online) Journal homepage: http://www.tandfonline.com/loi/inan20

# Health effects of selected nanoparticles in vivo: liver function and hepatotoxicity following intravenous injection of titanium dioxide and Na-oleate-coated iron oxide nanoparticles in rodents

Katarina Volkovova, Richard D Handy, Marta Staruchova, Jana Tulinska, Anton Kebis, Jana Pribojova, Olga Ulicna, Jarmila Kucharská & Maria Dusinska

**To cite this article:** Katarina Volkovova, Richard D Handy, Marta Staruchova, Jana Tulinska, Anton Kebis, Jana Pribojova, Olga Ulicna, Jarmila Kucharská & Maria Dusinska (2015) Health effects of selected nanoparticles in vivo: liver function and hepatotoxicity following intravenous injection of titanium dioxide and Na-oleate-coated iron oxide nanoparticles in rodents, Nanotoxicology, 9:sup1, 95-105

**To link to this article:** http://dx.doi.org/10.3109/17435390.2013.815285

Accepted online: 13 Jun 2013.

http://informahealthcare.com/nan
ISSN: 1743-5390 (print), 1743-5404 (electronic)

Nanotoxicology

Nanotoxicology, 2015; 9(S1): 95–105
 DOI: 10.3109/17435390.2013.815285

informa
healthcare

# Health effects of selected nanoparticles *in vivo*: liver function and hepatotoxicity following intravenous injection of titanium dioxide and Na-oleate-coated iron oxide nanoparticles in rodents

Katarina Volkovova[1], Richard D Handy[3], Marta Staruchova[1], Jana Tulinska[1], Anton Kebis[1], Jana Pribojova[1], Olga Ulicna[2], Jarmila Kucharská[2], & Maria Dusinska[4]

*[1]Slovak Medical University, Bratislava, Slovakia, [2]Comenius University, Bratislava, Slovakia, [3]School of Biomedical and Biological Sciences, Plymouth University, Plymouth PL4 8AA, UK and [4]NILU-Norwegian Institute for Air Research, Kjeller, Norway*



**Abstract**

The study determined the effect of intravenous administration of acutely toxic or sub-lethal doses of Na-oleate-coated $Fe_3O_4$ (OC-$Fe_3O_4$) nanoparticles (NPs) on liver structure and function in Wistar rats, compared to titanium dioxide ($TiO_2$) NPs and saline-injected controls. The acute study, using a modified OECD 425 progressive dosing procedure, found $LD_{50}$ values of 59.22 and 36.42 mg/kg for $TiO_2$ and OC-$Fe_3O_4$ NPs, respectively. In the sub-lethal study, rats were either injected with saline (negative controls), a sub-lethal reference (0.592 mg/kg$TiO_2$ NPs, equal to 1% of $LD_{50}$ on a body weight basis) or OC-$Fe_3O_4$ NPs in doses equivalent to 0.1, 1 or 10% of the $LD_{50}$, respectively (corresponding to 0.0364, 0.364 and 3.64 mg $Fe_3O_4$/kg body weight). Animals were sampled 24 h, 1, 2 and 4 weeks post-injection for adverse effects. Mitochondrial respiration was significantly increased 2 weeks after injection of 10% OC-$Fe_3O_4$ NPs compared to controls, but the effect was transient. Cholesterol and triacylglycerol concentrations in the liver tissue did not increase in any treatment. There were some disturbances to antioxidant enzymes after OC-$Fe_3O_4$ NPs treatment in the livers of animals 1 week post-exposure; with the most sensitive changes occurring in glutathione peroxidase (GPx) and glutathione *S*-transferase (GST) activities. Lipidosis and mild necrosis with changes in sinusoid space were also observed in histological sections of the liver. Overall, these data suggest that the liver likely retains functional integrity with acute and sub-lethal doses of OC-$Fe_3O_4$ NPs, albeit with some stimulation of redox defences and evidence of some tissue injury.

**Keywords**

*in vivo* nanotoxicology, Na-oleate-coated $Fe_3O_4$, $TiO_2$ nanoparticles, liver toxicity

**History**

Received 30 January 2013
Accepted 5 June 2013
Published online 29 April 2015

## Introduction

The present study reports some *in vivo* experiments conducted as part of the NanoTest project (http://www.nanotest-fp7.eu/). The main goal of the project was to develop alternative methods and high-throughput testing strategies using *in vitro* and *in silico* approaches to assess the toxicological profile of nanoparticles (NPs) used in medical diagnostics. This requires validation by collecting some *in vivo* data to compare with the *in vitro* and *in silico* modelling (reported elsewhere in this volume). Na-oleate-coated $Fe_3O_4$ (OC-$Fe_3O_4$) NPs were chosen for the present *in vivo* study because toxicity of this NP was demonstrated during *in vitro* experiments (Guadagnini et al. 2015). In keeping with the ethical principles of reduction, refinement and replacement (the 3Rs), the experimental design avoided conducting multiple toxicity tests with iron (Fe) salts, where the iron-overload toxicity and molecular biology of dissolved Fe is already well known (Aisen et al. 2001; Eaton & Qian 2002). Instead, the design included titanium dioxide ($TiO_2$) NPs as a benchmark because this is a more widely used NP where some information on systemic toxicity and biochemical effects on the liver is known (e.g. rodents; Wang et al. 2007; Umbreit et al. 2012; fish liver; Federici et al. 2007), and a no added NP control (vehicle only). It was not the purpose of this study to compare Fe NPs with dissolved Fe metal salts, but instead to provide *in vivo* data to support the replacement goals of the NanoTest project.

The present study used an intravenous (i.v.) route of exposure to reflect the likely medical applications of Fe NPs in medical imaging (Kim et al. 2001), where it is proposed that the NPs are given as bolus injection into the vein of patients. NPs directly injected into the blood for medical purposes are likely to end up in the liver. The notion of first-pass metabolism by the liver is well known. It has also been reported that, once inside the circulation, NPs are recognised by macrophages and are phagocytosed (Rømert et al. 1993; Sadauskas et al. 2007). Macrophages in the liver constitute a major pool of the total number of macrophages in the body. The Kupffer cells have been found to be central to the clearance of circulating NPs from the blood and their staggering ability to accumulate the circulating NPs has been proved in several studies (Rømert et al. 1993; Sadauskas et al. 2007; Iversen et al. 2013).

Dissolved Fe is well known for its redox chemistry, catalysing the Haber–Weiss reaction to generate superoxide inside cells, and the dietary uptake of dissolved Fe also involves reductions of

Correspondence: Katarina Volkovova, Slovak Medical University, Limbova 12, 833 03 Bratislava, Slovakia. E-mail: katarina.volkovova@szu.sk

Fe(III) to Fe(II) by ferric reductase on the gut mucosa, with subsequent reoxidation to Fe(III) on release into the blood (Bury & Handy 2010). Fe overload in animals and humans is characterised by oxidative damage to the liver (Eaton & Qian, 2002; Carriquiriborde et al. 2004), and this is a potential theoretical concern for bolus injections of Fe NPs in human patients. However, experimental trials with rodents so far suggest that at least some forms of Fe NPs may be relatively inert, or at least do not cause lasting haematological disturbances (Sebekova et al. 2014; Iversen et al. 2013). However, the blood is only the first line of redox defence and the effects on the liver cells that form the central compartment for Fe metabolism need to be investigated.

Mitochondria under normal conditions (not pathological) are probably the most important cellular source of reactive oxygen species (ROS) (Boveris & Chance 1973; Turrens 1997; Brookes 2004). The single-electron chemistry of mitochondrial oxidative phosphorylation (ox-phos) generates ROS by default. These ROS have roles in both physiological cell signalling and numerous pathological situations. The primary ROS generated in the organelle is superoxide ($O_2^-$), which is then converted to $H_2O_2$ by spontaneous dismutation, or by superoxide dismutase (SOD). The primary factor governing mitochondrial ROS generation is the redox state of the respiratory chain (Lambert & Brand 2004) and the mild uncoupling of ox-phos, that is, proton ($H^+$) leak across the mitochondrial inner membrane (Brookes et al. 1998). There is a positive correlation between $H^+$ leak and lipid polyunsaturation (Porter et al. 1996). It is possible that polyunsaturated lipids *per se* modulate the activity of uncoupling proteins or other proteins by affecting parameters such as membrane fluidity. ROS-induced $H^+$ leak via lipid oxidation is also highly likely because superoxide preferentially oxidises mitochondrial lipids, and lipid peroxides have well-established effects on mitochondrial respiration (Cheremisina & Vladimirov 1975). Changes in the lipid storage pattern in the liver are also readily discernible from routine histological sections (Carriquiriborde et al. 2004). Mitochondrial function, oxidative stress, lipid metabolism and storage are therefore part of a well-known continuum that indicates adverse changes in the liver. However, this fundamental aetiology of liver dysfunction has never been demonstrated for a NP, and not for Fe NPs.

The aim of this work was, therefore, not only to provide the *in vivo* data needed to help validate *in vitro* and *in silico* alternatives to invasive toxicity tests but also to explore the effect of i.v. administered $TiO_2$ and OC-$Fe_3O_4$ NPs on liver mitochondria respiratory function, on oxidative stress parameters and to consider this in the context of possible histopathological changes in the liver tissue.

## Methodology

### Nanoparticles

The NPs used in this study are commercially available and were provided with physicochemical characterisation by the supplier, while some further characteristics (e.g. the size distribution by dynamic light scattering – NICOMP 370 submicron particle sizer, DSS, California, USA; pH analyses) were performed on request within the NanoTEST Consortium at the University of Venice (Sebekova et al. 2014).

$TiO_2$ NPs (P25 obtained from Evonik Degussa GmbH, Essen, Germany); were provided by Joint Research Center (Ispra, Italy). The following information was supplied with the dry powder: nominal primary particle size 15–60 nm, crystal structure reported as a mixture of anatase and rutile crystallites in a ratio of 70:30 or 80:20), > 99% purity, Brunauer–Emmett–Teller (BET) surface area 61 $m^2/g$. A stock solution was suspended in physiological solution containing 10% v/v of rat serum (Sigma), pH = 7.5, and sonicated (DynatechArtek 300, Manassas, VA, USA) for 15 min at 150 W in a tube with diameter of 9 mm. In this suspension, the $TiO_2$ NPs displayed bimodal size distribution, with peaks at 84 ± 8 (61% of NPs) and 213 ± 15 nm (Sebekova et al. 2014).

The OC-$Fe_3O_4$ NPs (7% v/v) were purchased from PlasmaChem GmbH (Berlin, Germany) and supplied as a dispersion with particles comprising ~7% w/v; the shape of the particles was oblong, crystal structure Spinel (octahedral), and the surface was coated with oleate micelle. The particles had >99% purity, with an average iron oxide particle core size of 8 ± 3 nm, hydrodynamic diameter of 14–15 nm (determined by dynamic light scattering), and zeta potential of −30 mV at pH 7. The size distribution for OC-$Fe_3O_4$ NPs was also bimodal, with peaks at 31 ± 4 and 122 ± 3 nm, and pH of 6. After heating to 38°C, the planned volume was pipetted and diluted with physiological solution. The sample was homogenised by manual shaking.

### Acute toxicity study

The study was conducted according to the guidelines for experimental studies using laboratory animals (86/609/EEC), after the approval by the State Veterinary and Food Control Agency in Bratislava (Slovakia). A total of 39 female outbred Wistar rats (aged 8 weeks, weight 205.5 ± 8.5 g mean ± SD) from Prague (VELAZ, s.r.o.) were used for the experiment. A total of 14 animals were used to establish the $LD_{50}$ for $TiO_2$ NPs, and 18 animals were used to test the $LD_{50}$ for OC- $Fe_3O_4$ NPs. Seven animals were removed from the experiment for different practical reasons, for example, difficulty with injections where the NPs were suspected to be injected paravenously or complications from the xylazine anaesthesia. Rats were housed two animals per cage, under constant room temperature and humidity, 12 h L:12 h D light cycles, with *ad libitum* access to tap water and standard rat chow (SP1, Top Dovo, Horné Dubové, Slovakia). After a period of resting and adapting to the husbandry conditions, NPs were administered by i.v., under xylazine anaesthesia to the rodents. The animals were monitored 1 h and 4 h after injection and every 24 h during the following 14 days. Each animal was individually dosed, and therefore individually monitored during the experiment. After death, the animals were carefully dissected to collect the organs for routine wax histology, and samples were transported to the University of Plymouth for examination.

The acute lethal toxicity test was performed according to OECD guidelines 425 (OECD 2008), except that i.v. administration was used. The test consisted of a single ordered dose progression in which animals were dosed, one at a time, at a minimum of 48 h intervals. The first animal received a dose a step (~3.2-fold) below the level of the best estimate of the $LD_{50}$. If the animal survived, the dose for the next animal was increased by 3.2 times the original dose; if it died, the dose for the next animal was decreased by a similar dose progression. Each animal had to be observed for up to 48 h before making a decision on whether and how much to dose the next animal. The rats were observed for mortality, body weight effects and clinical signs for 14 days after dosing. A combination of three stopping criteria were used (as describe in OECD 425; OECD 2008) to minimise the number of animals used for the test. Dosing was stopped when one of these criteria was satisfied at which time an estimate of the $LD_{50}$ and a confidence interval were calculated using the method of maximum likelihood for the test based on the status of all the animals at termination.

### Sub-lethal study design

The study was conducted according to the same ethical approvals above. Female outbred Wistar rats (aged 8 weeks,

weight 205.5 ± 8.5 g mean ± SD, $n = 160$ rats) obtained from Prague (VELAZ, s.r.o.) were used for the experiment. The purpose of the current study was to determine the sub-lethal effects of doses representing a fraction of the $LD_{50}$ value. The sub-lethal doses were calculated from the preliminary acute experiment above. Female outbred Wistar rats ($n = 160$ animals/treatment) were randomly allocated into five groups consisting of a negative control (saline vehicle only); a sub-lethal reference dose (reference control) of a NP of known toxicity (0.592 mg/kg $TiO_2$ NPs, equal to 1% of $LD_{50}$/kg body weight basis) and three groups receiving OC-$Fe_3O_4$ NPs in doses equivalent to 0.1, 1 or 10% of the $LD_{50}$, respectively (corresponding to 0.0364, 0.364 and 3.64 mg $Fe_3O_4$/kg body weight). Animals were then sampled 24 h after injection (1 day), 1, 2 and 4 weeks post-injection for adverse effects. The i.v. injections (one injection per animal) were performed under combined ketamine/xylazine anaesthetisation, and on sampling days, animals were humanely euthanised by exsanguination under ketamine/xylazine anaesthesia. Each treatment consisted of 32 animals ($n = 4$/time point), which were blood sampled and dissected for the major internal organs (only liver data are reported here). For biochemistry, fresh livers were either used immediately or snap frozen in liquid nitrogen and stored frozen at −80°C.

### Measurement of respiratory functions in isolated mitochondria

Mitochondria were isolated from freshly excised livers by differential centrifugation as described by Hogeboom (1955), with some modification. The isolation medium was prepared, according to Sammut et al. (1998), with the following modification: it contained 225 mmol/l mannitol, 75 mmol/l sucrose and 0.2 mmol/l Titriplex III. The liver was minced in the isolation medium (pH 7.4) at 4°C and homogenised at a slow speed with rests in ice between burst, using a teflon to glass homogeniser. The homogenate was centrifuged at 700 *g* for 10 min to remove debris, then the supernatant was decanted and centrifuged at 5600 *g* for 10 min. The mitochondrial pellet was washed twice with isolation medium. The resulting pellet was then resuspended in the same medium to a final protein concentration of 20–40 mg/ml. All procedures were performed at 4°C. Protein concentration in the washed mitochondria was determined, according to Lowry et al. (1951).

Respiratory function of mitochondria was determined using the voltamperometric method on an Oxygraph Gilson 5/6 H instrument (Gilson Medical Electronics Inc., Middleton, WI, USA) with the use of Clark oxygen electrode (Yellow Springs Instruments Co., Yellow Springs, OH, USA) at 30°C. The incubation medium was prepared as described by Rouslin & Millard (1980) with a modification: 12.5 mmol/l HEPES, 122 mmol/l KCl, 3 mmol/l $KH_2PO_4$, 0.5 mmol/l Titriplex III and 2% dextran. Glutamate/malate at 2.5 mmol/l concentration for both was used as substrate for nicotinamide adenine dinucleotide (NAD). For assessing stimulated oxygen consumption, 500 nmol of adenosine diphosphate (ADP) was added.

The following parameters were determined in the liver mitochondria: oxygen consumption after stimulation by ADP (QO2(S3)) expressing the velocity of oxygen consumption by mitochondria in the presence of ADP and substrate; the rate of basal oxygen uptake by mitochondria without ADP – state 4 (QO2(S4)) denotes how fast oxygen is used by mitochondria in the presence of substrate only and the rate of ox-phos (OPR) (rate of adenosine triphosphate [ATP] production). Subsequently, the Respiratory Control Index (the ratio of state 3 to state 4) was calculated as an indicator of mitochondrial membrane integrity. Similarly, the coefficient of ox-phos (ADP:O) was calculated as an indicator of coupling of oxidation with phosphorylation.

### Biochemical analysis of liver homogenates

The potential for NPs to cause oxidative stress in the liver was evaluated by several biochemical approaches. These included determination of lipids that might be sensitive to oxidative stress (cholesterol and triacylglycerol) as well as reduced and oxidised forms of co-enzyme Q (CoQ). In addition, antioxidant enzyme activities and the malondialdehyde (MDA) product of lipid peroxidation were also measured in liver homogenates. Triglyceride concentrations in the liver were determined by the modified method of Jover (1963). Liver tissue (100 mg) was homogenised and extracted in chloroform–methanol (2:1). The interfering phospholipids were removed by absorption from the liver extract on silica gel. Purified extracts were evaporated and triglycerides were hydrolyzed with potassium hydroxide. Released fatty acids were removed by extraction into heptane. Finally, the released glycerol was oxidised by periodic acid, and after the reaction with phenylhydrazine hydrochloride and potassium ferricyanide, a coloured complex was spectrophotometrically measured at 530 nm.

Cholesterol was determined by the modified method of Abell et al. (1952). Liver tissue (100 mg) was homogenised in chloroform–methanol mixture (1:1). After lipid extraction, the Liebermann–Burchard colorimetric assay was used for the detection of cholesterol. Cholesterol concentrations were spectrophotometrically determined at 650 nm.

Oxidised and reduced forms of CoQ ($CoQ_{9\text{-ox}}$ and $CoQ_{9\text{-red}}$) were measured by a high-performance liquid chromatography (HPLC) method with spectrophotometric detection (Lang et al. 1986). The liver tissue (∼100 mg) was homogenised using an Ultra-Turrax in 1 ml of redistilled water with an addition of 50 µl of butylhydroxytoluene (BHT, 10 mg/L ml of 99.9% ethanol). The homogenate was extracted by hexane–ethanol mixture (5/2, v/v) with an addition of 1 ml of 0.1 M sodium dodecyl sulphate for 5 min. Liver mitochondrial suspension (100 µl) was extracted with an addition of 20 µl of BHT. The collected organic layers were evaporated under nitrogen (Termovap, 50°C) and the residues taken up in ethanol and injected to the HPLC column SGX C18, 7 µm (Tessek Ltd, Czech Republic). The mobile phase consisted of methanol/acetonitril/ethanol (6/2/2, v/v/v, Merck, Germany). The concentrations of compounds were spectrophotometrically detected using external standards (Sigma, Germany): tocopherols at 295 nm and CoQ at 275 nm. Data were collected and processed using CSW32 chromatographic station (DataApex Ltd, Czech Republic).

An aqueous phase buffer was used for the preparation of liver homogenates for antioxidant enzymes and MDA determination. Briefly, 100 mg of frozen liver tissue was homogenised in 1 ml of ice cold distilled water (10% w/v) using an Ultra-Turrax T8 homogeniser (IKA Labortechnik), set at 5000/min for 3 times 10 sec. The crude homogenate was centrifuged (1000 *g*) at 4°C for 10 min to remove debris, and the resulting supernatant diluted to 0.01% w/v of the original liver weight. Activity of glutathione peroxidase (GPx) was determined by a kinetic method, according to Paglia & Valentine (1967); the method is based on the ability of GPx to catalyze the oxidation of reduced glutathione (GSH) into oxidized glutathione (GSSG). The amount of GSSG is measured using glutathione reductase, and the reaction involves using nicotinamide adenine dinucleotide phosphate (NADPH). The amount of consumed NADPH is detected as a decrease of absorbance at 340 nm.

The activity of glutathione *S*-transferase (GST) was assessed by a kinetic method, according to Habig et al. (1974); the reaction

mixture contained 0.1 mol/l potassium phosphate buffer and 0.1 mol/l reduced glutathione. 1-chloro-2,4-dinitrobenzene was used as substrate (10 mmol/l). To minimise any non-enzymatic reaction, the measurements were conducted at 25°C and pH 6.5. The difference in absorbance was measured at 340 nm before and after the total enzymatic change of the substrate into product. Concentration was calculated from millimolar extinction coefficient for 1-chloro-2,4-dinitrobenzene conjugate at 340 nm (9.6).

The activity of SOD was estimated by a commercial test kit (Randox Lab. Ltd, Grumlin, UK). The method employs xanthine and xanthine oxidase to generate superoxide radicals which react with 2-(4-iodophenyl)-3-(4-nitrophenol)-5-phenyltetrazolium chloride (I.N.T.) to form a red formazan dye. The SOD activity is then measured by the degree of inhibition of this reaction. One unit of SOD causes a 50% inhibition of the rate of reduction of I.N.T. under the conditions of the assay. Catalase (CAT) activity was spectrophotometrically measured by a modified method of Cavarocchi et al. (1986). Briefly, the sample (50 µl of 1000 times diluted homogenate) was incubated for 10 min at 25°C with 0.01 mol/l potassium phosphate buffer, pH 7.8, which contained the substrate (0.285 mmol/l $H_2O_2$). Concentration of the remaining substrate in the reaction mixture was assessed at 505 nm by using the mixture for determination of $H_2O_2$. This mixture contained 3 mmol/l 4-aminoantipyrine, 0,1% water solution of phenol and 10 µl of peroxidase (2500 U/ml). Concentration of the remaining substrate was calculated from calibration curve.

Lipid peroxidation was assessed by measuring the concentration of MDA in the homogenates using a modified HPLC method (Wong et al. 1987), which involved first conjugating MDA with thiobarbituric acid (TBA), isolation of the MDA–TBA adduct by HPLC and detection by fluorimetry. Briefly, 50 µl of the aqueous supernatant above was added to a glass tube containing 750 µl of 0.44 mol/l phosphoric acid, 250 µl of 4.42 mmol/l TBA solution and 450 µl distilled water. After vortexing, the solution was incubated in a water bath at 100°C for 1 h, then cooled on ice. The MDA–TBA adduct was stable in the acidic pH of the media. Then, 500 µl of each sample was added into a tube containing 500 µl of methanol–NaOH solution (1 mol/l). The resulting mixture was then briefly vortexed and then centrifuged (11,300 *g*) for 3 min. HPLC was performed by adding 50 µl of the resulting supernatant to a Lichrospher 100 RP-18 column (125 × 4 mm I.D., 5 µm, Merck). The mobile phase consisted of potassium phosphate buffer (50 mmol/l, pH 6.8) and analytical grade methanol (60/40, v/v – mixture ratio of phosphate buffer and methanol). The TBA–MDA adduct was monitored by fluorescence (excitation wavelength, 532 nm; emission wavelength, 553 nm) on a Jasco 920 detector.

### Liver histology

Histological examinations were performed as described in Al-Bairuty et al. (2013), with minor modifications. Livers were examined from both the acute and sub-lethal experiments. For the acute lethal experiment, livers were collected after each animal was sacrificed at the appropriate time point. For the sub-lethal study, livers were collected for histology at each time point (5–8 livers from each treatment/time point). Livers were fixed for at least 2 weeks in buffered formal saline (250 ml 40% formaldehyde, 10 g $NaH_2PO_4.1\ H_2O$, 16.5 g $NaH_2PO_4$ (anhydrous), diluted to 2.5 L with distilled water and buffered to pH 7.2). Tissues were processed into wax blocks, and transverse sections (7–8 µm sections) were cut from each animal. Slides were stained with Mallory's trichrome. Photographs were taken using an Olympus Vanox – T microscope connected to an Olympus digital camera (C-2020 Z). Subsets of slides were independently scored to check for observer bias (this was negligible). Slides were also processed in batches containing controls and treatments were conducted to eliminate staining artefacts (SAs). Quantitative histological measurements were made. Fractional areas of the proportions of hepatocytes area and sinusoid space in the liver tissues were manually counted from a randomly selected area on a section from each animal (image) using the point counting method of Weibel et al. (1966), where the fractional volume (area) $V_i = P_i/P_T$ and $P_i$ is the number of points counted, $P_T$ is the total number of points on the counting grid.

### Statistical analysis

For the acute study, software AOT 425 StatPgm (http://www.epa.gov/oppfead1/harmonization) was used for the progressive calculation of the median lethal dose and to inform on the stop criteria in each acute toxicity test. Curve fitting of injected dose with survival time was performed using SigmaPlot version 12.2. Data from quantitative histology were not statistically analysed as the OECD 405 test design has insufficient replicates at each dose to conduct any useful analysis.

For the sub-lethal experiment, SPSS version 13.0 (SPSS Inc., Chicago, IL, USA) software was used for statistical analysis of all biochemistry and mitochondrial function data. Independent samples (unpaired) student's *t*-test was used to test for significant differences for normally distributed data, Mann–Whitney U test for not-normally distributed data. Differences with $p < 0.05$ were considered to be statistically significant. Data from quantitative histology were analysed using StatGraphic Plus version 5.1. One way analysis of variance (ANOVA) was used to identify dose–effects within the Fe NP treatments. The least squares difference *post hoc* test was used to identify differences between doses or between time-effects, where appropriate. Bartlett's test was used to check the validity of each ANOVA. In addition, two-way ANOVA was used to check for treatment × time effects in the data. The student's *t*-test was also sometimes used to investigate the differences between the pairs of data, where appropriate, such as comparing the 1% reference $TiO_2$ treatment with the equivalent OC-$Fe_3O_4$ NP treatment. For multiple comparisons with non-parametric data, the Kruskal–Wallis test was used for data that could not be transformed or the non-parametric Mann–Whitney U test was used as appropriate for pairs of data. All statistical analysis used the default 5% rejection level.

## Results

### Acute study

After single i.v. injection to adult rats, the $LD_{50}$ for $TiO_2$ NPs was established to be 59.22 mg/kg with a confidence interval from 55 to 70 mg/kg. For OC-$Fe_3O_4$ NPs, the $LD_{50}$ was 36.42 mg/kg with a confidence interval (0–20,000 mg/kg). The end of the experiment was also predicted by the software, when at dose 44 mg/kg, one animal survived and two died and at dose 35 mg/kg one animal survived and one died. Experimental modelling showed that continuing the study with additional animals would not improve the robustness of the statistical significance. The relationship between injected dose and the time of survival is shown (Figure 1) for animals that died within 2-week observation period. In general, the expected trend of decreasing survival time with increasing dose was observed. However, there was some inter-animal variability. For example, one animal injected with 139 mg/kg $TiO_2$ NPs survived until the end of the experiment (still alive at week 2 or 336 h post-injection), while another animal injected with the same dose survived only 10 h. Both animals injected with 55 mg/kg $TiO_2$ survived suggesting the acute toxicity threshold was somewhere between this dose and the next highest used (70 mg/kg). For OC-$Fe_3O_4$ NPs, two out of four

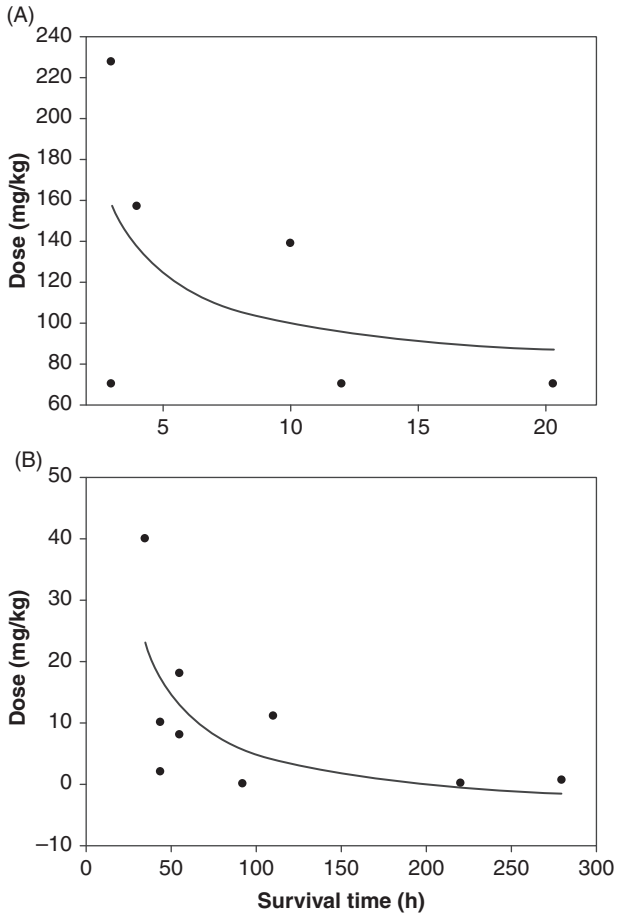


Figure 1. Relationship between dose and survival time in rats that were i.v. injected with a single acute treatment of (A) $TiO_2$ NPs or (B) OC-$Fe_3O_4$ NPs. Each data point is a single animal and curves were fitted using SigmaPlot 12.2 to an inverse first order polynomial fit. For $TiO_2$ NPs: $y = 74.0 + (252.2/x)$, $r^2 = 0.26$, $n = 6$ rats. For OC-$Fe_3O_4$ NPs: $y = -0.51 + (981.9/x)$, $r^2 = 0.49$, $n = 10$ rats. Some animals that survived for 2 weeks and were subsequently euthanised for histology are not included in the curve fits.

animals injected with 44 mg/kg survived, and one of two animals injected with 35 mg/kg survived, while the other died at 10 h post-injection.

The cause of death was not acute liver injury as the livers from the animals showed only mild or more moderate diffuse necrosis and some mild evidence of lipidosis, with some areas of normal cells (Figure 2). Blood vessels (BVs) and sinusoids were generally intact in all the animals examined and, for example, perivenular bleeding was not observed. There were no obvious signs of treatment-dependent changes in the proportional area of sinusoid space (ranging from 6 to 14% across all the animals examined). However, the red cells in the sinusoids were eosinophilic, and this was different from the occasional SA (condensed haematoxylin, not in the sinusoids) observed in one animal from the 139 mg/kg $TiO_2$ injection. Notably, granular deposits were observed in macrophages in the sinusoids, being present in the livers of all the animals examined that died regardless of the type of nanomaterial injected, but was much less evident or absent in the animals surviving the 55 mg/kg $TiO_2$ treatment.

### Sub-lethal injection study

There were no treatment-dependent mortalities in the sub-lethal study, although a range of biological effects were observed.

### Mitochondrial functions

Single i.v. administration of either type of NP or the vehicle controls had no statistically significant effect on ADP-stimulated respiration rate ($QO_2$ (S3)) 24 h after the injection ($p > 0.05$) with values ranging from 100.65 ± 10.07 (control), 96.57 ± 4.45 (1% reference dose $TiO_2$), and 99.62 ± 6.43 to 109.05 ± 7.99nAtO.mg prot.$^{-1}$.min$^{-1}$ for the lowest to highest OC-$Fe_3O_4$ NP treatments. However, there was a transient increase in the ADP-stimulated respiration rate to 134.97 ± 5.19nAtO.mg prot.$^{-1}$.min$^{-1}$ at week 2 in the highest OC-$Fe_3O_4$ NP treatment (statistically significant increase relative to controls, $p = 0.007$), but this difference was lost by the end of the experiment (week 4) with values returning to control levels (data not shown). Similarly, there were only minor changes in the basal respiration rate ($QO_2$ (S4)), with a transient but statistically significant increase ($p = 0.02$) to 14.86 ± 0.99nAtO.mg prot.$^{-1}$.min$^{-1}$ in the 10% equivalent dose of OC-$Fe_3O_4$ NP treatment from the control value of 11.07 ± 1.04 nAtO.mg prot.$^{-1}$.min$^{-1}$ at week 2 but with this difference being lost by week 4 (data not shown). OPR also showed a transient rise in the same treatment at the same time point ($p = 0.014$) – increasing to 368.73 ± 14.95 from the control value of 298.50 ± 19.63 nmolATP.mg prot.$^{-1}$. min$^{-1}$ at week 2. No other significant differences in OPR were observed (data not shown). No significant differences were detected in the calculated coefficient of ox-phos, which is indicator of coupling of oxidation with phosphorylation or in S3:S4 ratio – a parameter of mitochondrial membrane integrity was detected between the groups at any time interval after exposure. They were in the range between 8.38 ± 0.52 and 10.18 ± 0.40. There were no changes in the concentrations of the oxidised form of $CoQ_{10}$ in isolated liver mitochondria during the experiment (data not shown), except at week 4 post-injection, where the concentration was significantly lower ($p = 0.049$) in the 0.1% equivalent dose of OC-$Fe_3O_4$ NPs at 4 weeks, with the value decreasing to 4.65 ± 2.83 nmol/mg protein compared to the control (6.73 ± 2.65 nmol/mg protein). No significant differences in oxidised or reduced forms of $CoQ_9$ in isolated liver mitochondria were recorded between the groups at any other time interval after exposure.

There were no significant differences in cholesterol or triacylglycerol (TAG) concentrations in the liver tissue between the groups (data not shown).

There were no clear time- or treatment-dependent effects on the activities of GPx or GST (Figures 3A and B), except for a transient change in the liver homogenates at 1 week post-exposure where GPx activity was significantly lower ($p = 0.044$) and the activity of GST was significantly higher ($p = 0.040$) in the group with the highest concentration of OC-$Fe_3O_4$ NPs compared to controls. Similarly, there were no clear time- or treatment-dependent changes in the MDA concentrations in liver homogenates (Figure 3C). However, there was a statistically significant decrease in MDA concentrations at day 1 post-exposure in the group with the lowest concentration of OC-$Fe_3O_4$ NPs compared to controls (Figure 3C). There were no significant differences in the activities of SOD and CAT in liver tissue homogenates between the groups at any time interval after exposure to NPs. SOD activity was the highest in the group with 1% OC-$Fe_3O_4$ NPs compared to controls (4.140 ± 0.837 vs. 3.318 ± 0.349 μmol/min/mg protein) 1 day post-exposure. Activity of CAT was the highest in the group with the lowest concentration of OC-$Fe_3O_4$ NPs compared to controls (16.13 ± 1.41 vs. 14.70 ± 2.25 μmol/min/mg protein).

### Liver histology following sub-lethal injections

Example images of the livers from rats at day 1 post-injection are shown in Figure 4. Overall, the unexposed controls were normal,

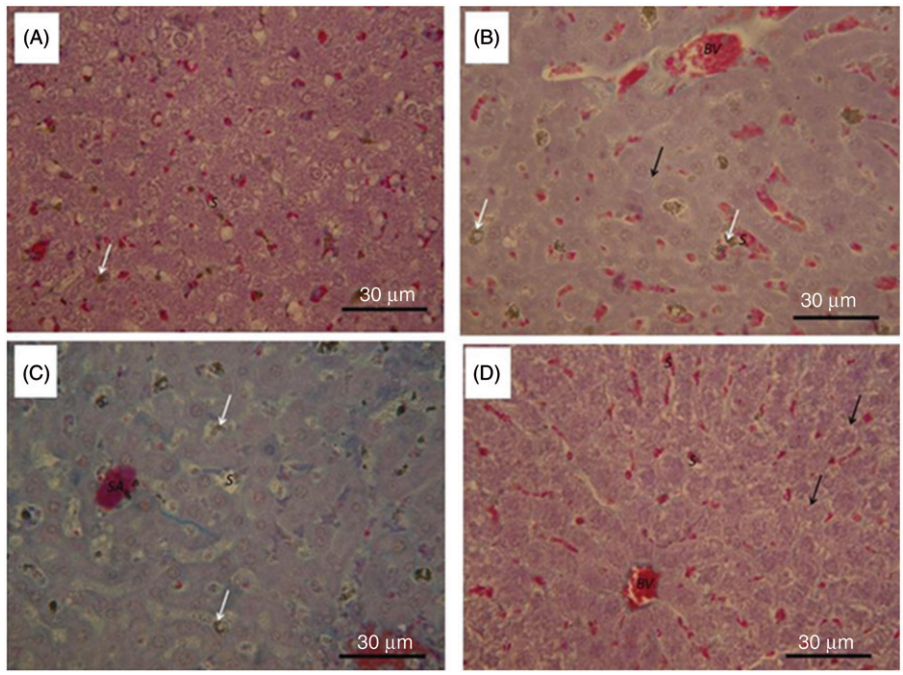


Figure 2. Examples of liver histology from the acute study with rats injected with (A) 220 mg/kg OC-$Fe_3O_4$ NPs and surviving for about 5 min, (B) 110 mg/kg OC-$Fe_3O_4$ NPs and surviving for 11 h, (C) 139 mg/kg $TiO_2$ NPs and surviving for 10 h, (D) 55 mg/kg $TiO_2$ and still alive at the end of the experiment (2 weeks post-injection). Note that the mild and diffuse necrosis in all the specimens, evidence of lipidosis in a few cells (black arrows) and granular deposits (assumed hemosiderin deposits) in macrophages (white arrows) are located mainly in the sinusoid space (S). Note the occasional SA and more basophilic nature of the staining with the higher $TiO_2$ NP injection, and the intact BV with endothelium at the lower $TiO_2$ dose. Sections (7–8 µm) were stained with Mallory's trichrome.

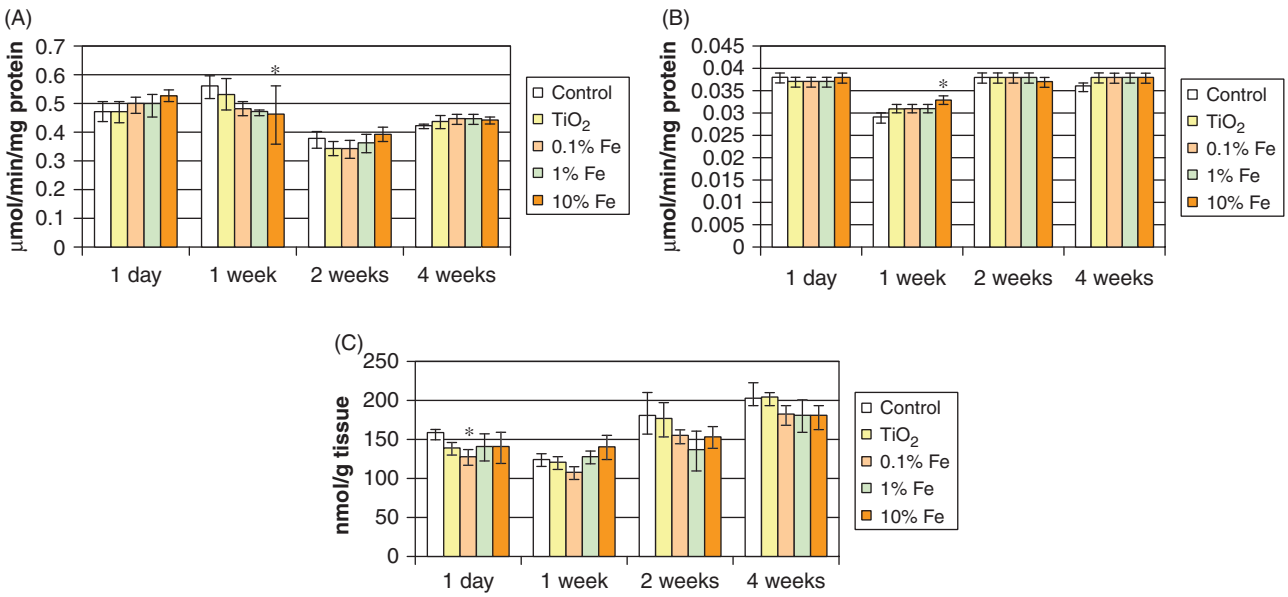


Figure 3. The effect a single sub-lethal i.v. injection of OC-$Fe_3O_4$ NPs on (A) GPx activity, (B) GST activity and (C) MDA concentrations in liver homogenates. Livers were collected at day 1 and 1, 2 and 4 weeks post-injection for biochemistry. Data are means ± S.D., $n = 8$ rats/treatment at each time point; *statistically significant difference from the control within treatment and time point.

but there were some minor injuries associated with both types of NPs, which improved over time. The livers of control animals at day 1 post-injection showed normal histology (all five animals examined) with well-defined nuclear membranes, a condensed nucleolus and with normal granular diffuse chromatin. Hepatocytes showed apparent glycogen storage space, although the livers were lean (as expected from young rats on maintenance rations). The sinusoid space appeared normal, and BVs where observed showed a normal endothelium. There was no evidence of perivenular bleeding, fatty change, extensive intracellular lipidosis or vacuoles in the parenchyma. Controls examined at week 1 through to week 4 showed similar normal architecture.

The $TiO_2$ treatment caused some minor pathology, which improved slowly but had not fully recovered by 4 weeks post-injection. At day 1 post-injection, six of seven of the specimens examined showed evidence of either diffuse definition of some of the cell membranes and some slight loss of definition to the nucleus, indicating a mild diffuse necrosis. In addition, four of seven livers showed some mild lipidosis and the occasional vacuole formation in cells. This was only evident in livers with apparent glycogen space, and lean livers (three of seven livers) showed no lipidosis. Where BVs were observed, the endothelium was intact. The mild necrosis (four of seven animals) continued by week 1 post-exposure and was still mildly present at week 4 (all six animals examined), with four of six animals examined showing some residual lipidosis.

Overall, the exposure to OC-$Fe_3O_4$ NPs caused the most liver pathology at day 1 post-exposure, and there was a clear dose-dependent increase in the injuries with generally mild effects at the 0.1% equivalent dose compared to the occasional area with

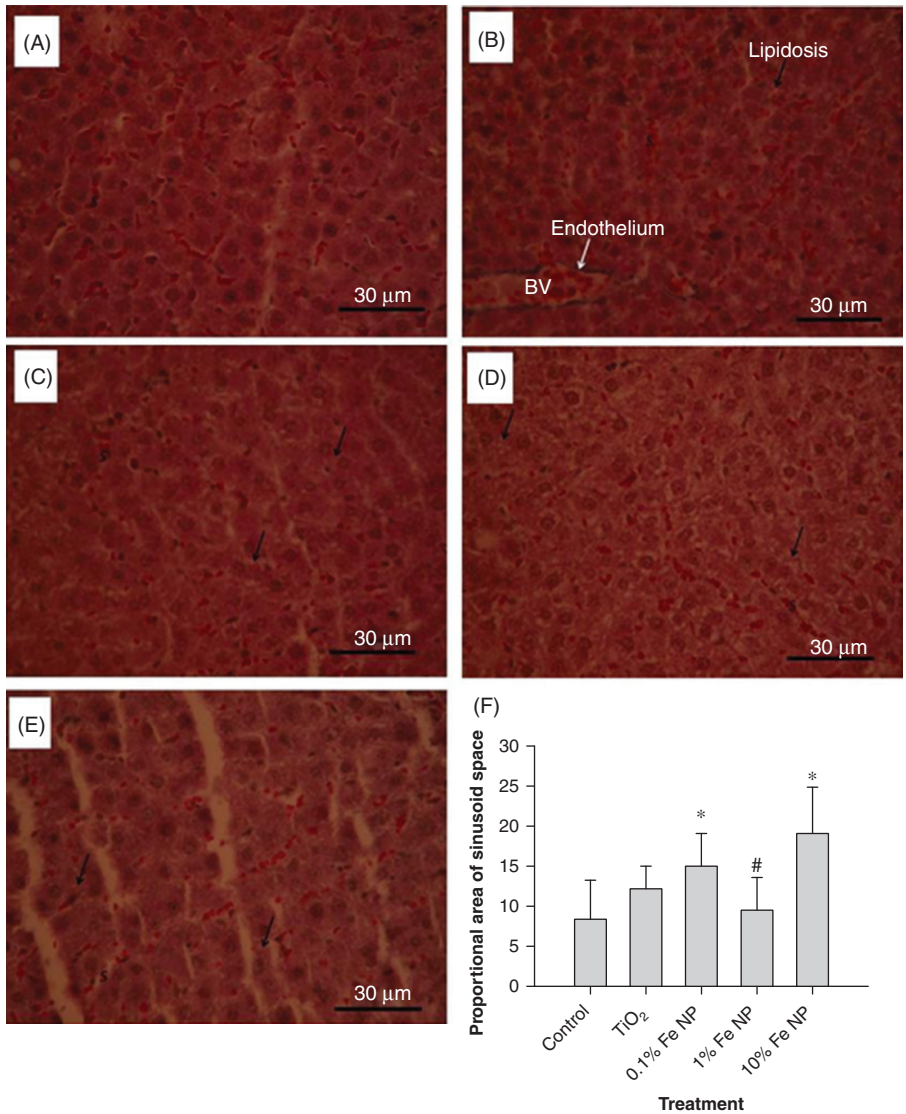


Figure 4. Histological sections of rat liver 1 day after a single sub-lethal i.v. injection of OC-$Fe_3O_4$ NPs. (A) control (vehicle only), (B) a reference $TiO_2$ NP dose equivalent to 1% of the $LD_{50}$ and doses of OC-$Fe_3O_4$ NPs equivalent to (C) 0.1%, (D) 1% and (E) 10% of the $LD_{50}$. Note the normal morphology of the controls, but more diffuse morphology and early signs of mild lipidosis (black arrows) in the $TiO_2$ treatment, but normal endothelium (white arrow) of the BV and sinusoid space (S). The lipidosis and diffuse mild-to-moderate necrosis progressed with increasing doses of the OC-$Fe_3O_4$ NPs. Panel (F) shows the proportion of sinusoid space in each treatment at day 1. Data are means ± S.D. $n = 5$–8 rats/treatment; *statistically significant difference from the control (ANOVA, $p < 0.05$); #statistically significant difference to the other Fe NP treatments.



moderate or worse loss of liver architecture in the 10% equivalent dose of the Fe NPs. However, the injuries showed some improvement by week 1 and in most cases completely recovered by week 4. At day 1 in the 0.1% equivalent dose of OC- $Fe_3O_4$ NPs, six of eight livers examined showed a mild or moderate diffuse necrosis. In all the livers with apparent glycogen space, there was also a mild lipidosis (three of eight animals). The animals from the 1% equivalent dose showed a greater incidence of necrosis (six of seven showing moderate areas of necrosis), and four of seven showed lipidosis that was worse than the 0.1% Fe-NP treatment. The pathology was greatest at day 1 in the highest Fe concentration. The livers of two of five animals examined showed a diffuse loss of architecture (wide-spread but moderate necrosis) with lipidosis. In the remaining three of five livers, the damage was slightly more severe. A quantitative analysis of the proportional of sinusoid space in the livers at day 1 post-injection showed that the sinusoid space had significantly increased (ANOVA, $p = 0.0045$) in the 0.1% and 10% equivalent dose of OC-$Fe_3O_4$ NPs compared to controls, with the highest Fe treatment showing the greatest increase in sinusoid space (Figure 4).

By week 1 post-injection, the livers from the 0.1% equivalent dose of Fe-NPs continued to show necrosis (all seven animals) and three animals also showed mild-to-moderate lipidosis. However, by week 2, this had improved and at week 4 only two of seven animals had a mild diffuse necrosis and five of seven were normal compared to time-matched controls. In the 1% equivalent dose at week 1, three of six animals showed moderate necrosis with lipidosis (three were normal), but this also improved over time with five of six animals examined being normal at week 2 and week 4. In the 10% equivalent dose mg/kg treatment, the pathology had improved compared to the animals at day 1, with all four specimens examined showing diffuse mild or moderate necrosis. In these animals, sinusoid space was discernible and BVs were intact. By week 4, the animals had recovered, with all five animals examined at the highest Fe NP concentration having normal histology.

## Discussion

This study provides one of the first detailed insights into the sub-lethal effects of known doses of OC-$Fe_3O_4$ NPs relative to the lethal concentration and compared to a reference dose of $TiO_2$ NPs. Overall, the data show that there are transient disturbances to enzymes involved in redox defences (GPx and GST) in the first week following sub-lethal injection, then later in week 2, some transient increases were detected in mitochondrial respiration (basal oxygen consumption and the OPRs) in the OC-$Fe_3O_4$ NPs group, without changes in cholesterol or triacylglycerol concentrations. The liver histology revealed some mild lipidosis due to $TiO_2$ NPs one day after injection, and progressive (dose-dependent) lipidosis with diffuse necrosis in the livers from the

OC-$Fe_3O_4$ NPs groups, but the livers showed recovery in most treatments by week 4 post-injection.

### Progressive dose method for the determination of acute toxicity

The OECD guideline 425 is an acute oral toxicity test (via oral gavage) that uses a progressive single dosing procedure to minimise the use of animals, while enabling an estimation of the median lethal concentration. In the present study, the design of the OCED 425 test had been followed, except that i.v. injection rather than oral gavage had been used to reflect the clinical application of the nanomaterials. The data analysis shows that this procedure will give lethal dose estimates, and the method gives the expected trend of increasing survival at the lower doses for both materials (Figure 1). This suggests that an i.v. modification of the OECD 425 test may be suitable for the acute testing of nanomaterials. Similar to our approach, Gajdosikova et al. (2006) also used this guideline for determining the $LD_{50}$ for i.v. administered $Fe_3O_4$ NPs in mice, finding an $LD_{50}$ in the range of 231–559 mg/kg of body weight, depending on the type of coating on the material. The $LD_{50}$ in the present study (36 mg/kg for OC-$Fe_3O_4$ NPs) is a little less for rats, and may be due to species difference, although the confidence intervals in both studies overlap.

One major concern of the progressive dose method is that the confidence intervals calculated by the software are not exact, and with typically low number of animals used in an acute test, the method should only be considered as a guide to indicate a range where the $LD_{50}$ may be found (OECD 2008). In cases, such as the $TiO_2$ experiment, where there was a clear dose where all the animals died and the next lowest dose where all the animals survived, the software will tend to generate reasonably tight confidence intervals (55–70 mg/kg in the present study for $TiO_2$ NPs). However in the OC-$Fe_3O_4$ NPs experiment, the confidence interval was very large (0–20,000 mg/kg) and this is related to a limitation of the computation method used in the OECD 425 test. At the two lowest doses used, some animals survived, but at the same doses some animals died. This uncertainty, while still meeting the stop criteria of the test, leads to an artefact in the confidence interval where the lower confidence interval is estimated at infinity (i.e. reported as zero) and often with a high upper confidence interval as well. This is a generic limitation of the test procedure and is recognised in the guidance notes (OECD 2008). It can be mathematically overcome by increasing the number of animals above and below the threshold for toxicity, but this solution would be in direct conflict with the original ethical drivers of minimising the use of animals that the test was designed to achieve. In the case of the present study for OC-$Fe_3O_4$ NPs, this problem relates only to identifying the outer limits of the confidence interval for all the data and does not mean the resulting $LD_{50}$ is of no scientific value; the software will still produce a lethality estimate around the median. However, the data should be interpreted with caution.

The results of the acute toxicity test also identified some inter-animal variability in mortality time that was not always explained by the exposure dose. During the study, several practical difficulties were encountered. At relatively high doses (close to the lethal dose), animals had to be injected with volumes often exceeding 0.5 ml, although this remained <5% of the blood volume (estimated blood volume of a 205 g rat is 11.9 ml), the procedure lasted more than 10 sec, so it was necessary to keep the animal under anaesthesia during the tail vein injection. Some necrosis/injury of peripheral tissue in the distal part of tail after injection did emerge after several days, suggesting some collapse or thrombosis of the BVs distally to the site of injection with high doses. However, this was a localised effect as internal organs, such as the liver, showed normal vasculature and sinusoid space (Figure 2).

The cause of death in the animals from the acute study cannot be deduced from the time to mortality measurements made in this modified version of the OECD 425 test. However, the absence of gross pathology in the livers, with generally normal sinusoids, only mild diffuse necrosis, and evidence of macrophage activity, suggests that liver failure is an extremely unlikely explanation.

### Sub-lethal effects of the $TiO_2$ NP reference dose

The study design of the sub-lethal experiment incorporated a reference dose of $TiO_2$ NPs equivalent to 1% of the lethal dose (an actual dose of 0.592 mg/kg $TiO_2$ NPs). Acute studies with i.v. injections of at least ten times the dose used here in rodents (e.g. van Ravenzwaay et al. 2009, 5 mg/kg body weight) show that systemically available $TiO_2$ NPs are mainly trapped in the liver (and spleen), thus confirming the importance of the liver as a target organ for i.v. injections. Similar observations have been made in fish injected with $TiO_2$ NPs with a trend of increasing Ti metal in the liver (Scown et al. 2009). The single i.v. administration of $TiO_2$ NPs did not induce any significant change in the parameters measured in the present study. Recently, Umbreit et al. (2012) injected mice with 56 mg/kg $TiO_2$ NPs and reported no major histological changes in the liver, apart from an expected macrophage infiltrate to deal with the NPs deposited in the tissue. Similarly, this study found relatively modest changes in liver histology with a $TiO_2$ injection (Figure 4), and with no statistically significant change in sinusoid space indicating that blood flow and/or fluid balance in the liver was also unaffected. Thus, overall, the reference $TiO_2$ dose behaved as expected and had no or limited effects on the parameters measured.

### Effects of OC-$Fe_3O_4$ NPs

The present study showed some transient effects of mitochondrial respiration, and there are some relatively well-known mechanisms for the effects of traditional dissolved forms of metals on the functions of mitochondria. These can include: (i) indirect effects through systemic hypoxia caused by respiratory injury or disturbances to the cardiovascular system (Watts et al. 1999) and (ii) direct interference of the dissolved toxic metal with respiratory coupling in the mitochondrial respiratory chain or the metal centres in the enzymes involved in the chain (e.g. Belyaeva & Korotkov 2003). In the present study, systemic hypoxia seems unlikely because the animals were not exposed via the lung. In addition, a previous report of blood function in the same animals used here showed no adverse effects on haematology or total concentrations of plasma Fe (Sebekova et al. 2014), although, injections of high doses of Fe NPs can produce a transient drop in mean arterial blood pressure in rats (10 mg/kg, Iversen et al. 2013). Respiratory chain uncoupling also seems unlikely since the homogenates demonstrated ADP-dependent stimulation of respiration and respiration rates did not decrease. Direct interference of dissolved Fe with copper (Cu) centres in enzymes such as SOD (Moody 1997) also seems unlikely, given that in dissolved iron toxicity the Cu is not displaced, and in the nano form, the dissolution rates of dissolved Fe from $Fe_3O_4$ NP are low (Sebekova et al. 2014). In addition, *in vitro* studies with $Fe_3O_4$ NPs (30–45 nm) on the neuro-2A cell line did not demonstrate a decrease in mitochondrial function (Jeng & Swanson 2006), thus supporting the findings here *in vivo*. Instead, the increase in oxygen consumption after stimulation by ADP, basal oxygen consumption and OPR (rate of ATP production) at week 2 is interpreted as a transient adaptive change to maintain mitochondrial respiration, following a brief period of mild oxidative stress the week before (see below). CoQ plays an important role in

mitochondrial bioenergetics in both the electron transport chain and proton translocation in order to power the proton motive gradient necessary for ATP synthesis (Villalba et al. 1995; Bhagavan & Chopra 2006). The $CoQ_9$ homologue is the dominant form of CoQ in rats. No significant differences in oxidised or reduced forms of $CoQ_9$ in isolated liver mitochondria were detected in this study, confirming that homeostasis was maintained. However, concentrations of the oxidised form of $CoQ_{10}$ in isolated liver mitochondria were significantly lower in the group with the lowest dose of OC-$Fe_3O_4$ NPs 4 weeks after exposure. This decrease was only of about 2 nmol/mg protein, and the reported $CoQ_{10}$ value of 4.65 nmol/mg protein was within the normal range expected in rat liver homogenates (e.g. about 1 nmol/mg protein, Kwong et al. 2002). This small change might be explained by increased activity of the Fe-dependent NADH CoQ reductase which replenishes the supply of the reduced form of CoQ; however, further experiments are needed to verify this suggestion.

Some metallic NPs are now known to cause oxidative stress (Schrand et al. 2010), and this has also been suggested as a mode of action for iron oxide NPs (in hepatocytes, Hussain et al. 2005; lung epithelial cells, Khan et al. 2012). The i.v. injections of Fe complexes affect the extent of weakly bound iron and thus the degree of oxidative stress. Toblli et al. (2011) showed that low molecular weight iron dextran and ferumoxytol caused renal and hepatic damage in normal rats, which was demonstrated by proteinuria and increased liver enzyme activities. Oxidative stress in these tissues was also implicated by higher MDA concentrations, increased antioxidant enzyme activities and a significant reduction in the reduced glutathione to oxidised glutathione ratio (Toblli et al. 2011). Similarly, Feng et al. (2011) found alterations of renal, hepatic and spleen functions, which were reflected by changes in a number of metabolic pathways including those involved in energy, lipid, glucose and amino acid metabolism after i.v. administration (25 mmol/l iron suspended in 0.9% saline) of ultra-small superparamagnetic particles of iron oxide. The present study, at much lower injected doses than those studies above, did not show any statistically significant changes in the MDA concentrations in the liver homogenates, but did show a transient increase of GST activity 1 week after the injection of OC-$Fe_3O_4$ NPs. GSTs carry out a wide range of functions in cells, including the removal of ROS during oxidative stress (Feng et al. 2011), the conjugation of reduced glutathione to electrophilic centres in Phase II reactions (Habig et al. 1974) and the reaction with numerous exogenous chemicals including environmental pollutants and oxidised biomolecules (Hayes & Pulford 1995). It is, therefore, not possible to specifically identify the specific mechanism of the GST increase in this study, but some oxidative stress seems likely, given the mild lipidosis in the livers (caused by lipid peroxidation).

A statistically significant decrease in the activity of GPx was also detected 1 week after the injection and was coincident with the liver pathology (Figure 4). GPx has roles in the detoxification of $H_2O_2$ (likely produced from hydroxyl radicals in Haber–Weiss reaction), and GPx activity is, therefore, expected to increase during ROS production. However, GPx activity is dynamic, and chemical antioxidants are regarded as the first line of defence inside the liver *in vivo* (vitamin E levels, glutathione concentrations). The absence of increases in MDA in the present study suggests that upregulation of GPx activity was not needed.

Liver pathology from Fe overload is well known and involves oxidative damage to the liver that may manifest as fatty change, leading to lipidosis (peroxidation of lipids in the tissue) and eventually to necrosis of the liver cells (Whittaker et al. 1996; Carriquiriborde et al. 2004). Ma et al. (2012) reported that the liver cells ''expanded'' and the liver sinus contracted with an intraperitoneal dose of 10 mg/kg of $Fe_3O_4$ NPs and found glutathione depletion in liver homogenates at doses of 40 mg/kg of the material. Unfortunately, Ma et al. (2012) did not perform quantitative histological measurements or use proper technical terms to describe the histology. They also reported a euthanasia method that would be ethically very unacceptable in the European Union (by ''having their eyes removed and blood drained'', Ma et al. 2012), and the latter would almost certainly lead to major artefacts in the liver histology during blood loss, such as collapse of the hepatic sinus. In the present study (Figure 4), OC-$Fe_3O_4$ NPs caused a dose-dependent lipidosis with some diffuse necrosis of the liver cells by day 1 and a concomitant increase in sinusoid space. This is most easily explained by oxidative stress associated with Fe exposure, and notably the nano form of Fe used here caused remarkably similar pathology to excess dietary iron sulphate. For example, Carriquiriborde et al. (2004) also showed aspects of fatty change with loss of glycogen and an increase in sinusoid space (also observed here, Figure 4). This suggests that either some dissolved Fe from the NP form or Fe NPs themselves were bioavailable to the liver cells or, more likely, that both forms of Fe cause liver injury via oxidative stress. Iversen et al. (2013) reported that magnetic resonance imaging and transmission electron microscopy showed accumulation of polyacrylic acid-coated $\gamma$-$Fe_2O_3$ NPs in liver cells 1 h after i.v. infusion of the NPs in mice, thus demonstrating that liver cells can take up intact Fe particles. In the present study, the recovery time of the liver in relation to the time course of GST also supports the latter hypothesis of oxidative injury, where improvement in the liver tissue mostly occurred after the increase in GST at week 1.

## Conclusions and clinical perspectives

Overall, the data reported in the present study suggest that the liver likely retains functional integrity with sub-lethal doses of OC-$Fe_3O_4$ NPs, albeit with some stimulation of redox defences and evidence of some tissue injury shortly after the injection. The absence of changes in liver cholesterol and triacylglycerol concentrations also support the notion of limited toxic effects. One of the potential clinical applications of $Fe_3O_4$ NPs is for enhancing nuclear magnetic resonance imaging (Kim et al. 2001) and like all new medicines or medical devices, a weight of evidence is needed to confirm that such Fe NPs are both safe and effective in animal models before progressing to clinical trials with human volunteers. The data so far (Sebekova et al. 2014, Iversen et al. 2013) suggest no lasting adverse effects on modest single injections of $Fe_3O_4$ NPs, and the subtle effects observed here should not be a barrier to further investigations on the medical applications of Fe NPs. For a prospective medicine, it is also important that ineffective or unsafe candidates are removed early on in the preclinical phase of drug development. This requires a battery of *in vitro* and *in silico* assays, and in keeping with the aims of the NanoTEST project, the data here, also provides some *in vivo* observations to support the interpretation of these alternative methods.

## Acknowledgements

Analyses of size distribution and pH of both types of NPs were done in University of Venice (by equipment NICOMP 370, submicron particle sizer, Nicomp International, Inc., New York, NY, USA). Michael Hockings and Lewis Young are thanked for their help in preparing the liver sections at Plymouth University. The authors acknowledge the support of the European Commission 7th Framework Programme for the NanoTEST project (Health-2007-1.3-4, Contract no: 201335). The work was also supported by EC FP7 QualityNano [INFRA-2010-1.131], Contract no: 214547-2, and EC FP7 NANoREG, [NMP.2012.1.3-3], Contract no: 310584.

## Declaration of interest

The authors report no conflicts of interest. The authors alone are responsible for the content and writing of the paper.

## References


Abell LL, Levey BD, Brodie BB, Kendall FF. 1952. A simplified method for the estimation of total cholesterol in serum and demonstration of its specificity. J Biol Chem 195:357–366.

Aisen P, Enns C, Wessling-Resnick M. 2001. Chemistry andbiology of eukaryotic iron metabolism. Int J Biochem Cell Biol 33:940–959.

Al-Bairuty GA, Shaw BJ, Handy RD, Henry TB. 2013. Histopathological effects of waterborne copper nanoparticles and copper sulphate on the organs of rainbow trout (Oncorhynchus mykiss). Aquat Toxicol 126: 104–115.

Belyaeva EA, Korotkov SM. 2003. Mechanism of primary Cd2+-induced rat liver mitochondria dysfunction: discrete modes of Cd2+ action on calcium and thiol-dependent domains. Toxicol App Pharm 192:56–68.

Bhagavan HN, Chopra RK. 2006. Coenzyme Q10: Absorption, tissue uptake, metabolism andpharmacokinetics. Free Rad Res 40:445–453.

Boveris A, Chance B. 1973. The mitochondrial generation of hydrogen peroxide: general properties and effect of hyperbaric oxygen. Biochem J 134:707–716.

Brookes PS, Buckingham JA, Tenreiro AM, Hulbert AJ, Brand MD. 1998. The proton permeability of the inner membrane of liver mitochondria from ectothermic and endothermic vertebrates and from obese rats: correlations with standard metabolic rate and phospholipid fatty acid composition. Comp Biochem Physiol B 119: 325–334.

Brookes PS, Yoon Y, Robotham JL, Anders MW, Sheu SS. 2004. Calcium, ATP and ROS: a mitochondrial love–hate triangle. Am J Physiol 287:C817–C833.

Bury NC, Handy RD. 2010. Copper and iron uptake in teleost fish. In: Bury N, Handy RD, editors. Surface chemistry, bioavailability and metal homeostasis in aquatic organisms: an integrated approach. Vol. 2. London: Essential Reviews in Experimental Biology, Society for Experimental Biology Press. pp. 107–127.

Carriquiriborde P, Handy RD, Davies SJ. 2004. Physiological modulation of iron metabolism in rainbow trout (Oncorhynchus mykiss) fed low and high iron diets. J Exp Biol 207:75–86.

Cavarocchi NC, England MD, O'Brien JF, Solis E, Russo P, Schaff HV, et al. 1986. Superoxide generation during cardiopulmonary bypass: is there a role for vitamin E? J Surg Res 40:519–527.

Eaton JW, Qian M. 2002. Molecular bases of cellular iron toxicity. Free Radical Biol Med 32:833–840.

Federici G, Shaw BJ, Handy RD. 2007. Toxicity of titanium dioxide nanoparticles to rainbow trout, (Oncorhynchus mykiss): gill injury, oxidative stress, and other physiological effects. Aquat Toxicol 84: 415–430.

Feng J, Liu H, Bhakoo KK, Lu L, Chen Z. 2011. A metabonomic analysis of organ specific response to USPIO administration. Biomaterials 32(27):6558–6569.

Gajdošíkova A, Gajdošík A, Koneracká A, Závišová A, Štvrtina S, Krchnárová V, et al. 2006. Acute toxicity of magnetic nanoparticles in mice. Neuro Endocrinol Lett 27(Suppl2):96–99.

Guadagnini R, Halamoda B, Walker L, Pojana G, Magdolenova Z, Bilanicova D, et al. 2015. Toxicity screenings of nanomaterials: challenges due to interference with assay processes and components of classic in vitro tests. Nanotoxicology 9(S1):13–24.

Habig WH, Pabst MJ, Jakoby WB. 1974. Glutathione Stransferases. The first enzymatic step in mercapturic acid formation. J Biol Chem 249: 7130–7139.

Hayes JD, Pulford DJ. 1995. The glutathione s-transferase supergene family: regulation of GST and the contribution of the isoenzymes to cancer chemoprevention and drug resistance. Crit Rev Biochem Mol Biol 30:445–600.

Hogeboom GH. 1955. Fractionation of cell components of animal tissues. In: Colowick SP, Kaplan NO, editors. Methods in enzymology. Vol. 1. New York: Academic Press Inc. pp. 16–19.

Hussain SM, Hess KL, Gearhart JM, Geiss KT, Schlager JJ. 2005. In vitro toxicity of nanoparticles in BRL 3A rat liver cells. Toxicol In Vitro 19: 975–983.

Cheremisina ZP, Vladimirov A. 1975. Effect of endogenous lipid peroxides on respiration in rat liver mitochondria. Biokhimiia 40: 242–247.

Iversen NK, Frische S, Thomsen K, Laustsen C, Pedersen M, Hansen PBL, et al. 2013. Superparamagnetic iron oxide polyacrylic acid coated γ-Fe2O3 nanoparticles do not affect kidney function but cause acute effect on the cardiovascular function in healthy mice. Toxicol Appl Pharm 266:276–288.

Jeng HA, Swanson J. 2006. Toxicity of metal oxide nanoparticles in mammalian cells. J Environ Sci Health A Tox Hazard Subst Environ Eng 41(12):2699–2711.

Jover A. 1963. Technique for the determination of serum glycerides. J Lipid Res 4:228–230.

Khan MI, Mohammad A, Patila G, Naqvi SAH, Chauhan LKS, Ahmad I. 2012. Induction of ROS, mitochondrial damage and autophagy in lung epithelial cancer cells by iron oxide nanoparticles. Biomaterials 33: 1477–1488.

Kim DK, Zhang Y, Voit W, Roa KV, Kehr J, Bjelke B, et al. 2001. Superparamagnetic iron oxide nanoparticles for bio-medical applications.Scripta mater. 44:1713–1717.

Kwong LK, Kamzalov S, Rebrin I, Bayne ACV, Jana CK, Morris P, et al. 2002. Effects of coenzyme Q(10) administration on its tissue concentrations, mitochondrial oxidant generation, and oxidative stress in the rat. Free Rad Biol Med 33:627–638.

Lambert AJ, Brand MD. 2004. Inhibitors of the quinone binding site allow rapid superoxide production from mitochondrial NADH: ubiquinone oxidoreductase (complex I). J Biol Chem 279: 39414–39420.

Lang JK, Gohil K, Packer L. 1986. Simultaneous determination of tocopherols, ubiquinols, and ubiquinones in blood, plasma, tissue homogenates, and subcellular fractions. Anal Biochem 157: 106–116.

Lowry OH, Rosenbrough UJ, Farr AL, Randall RJ. 1951. Protein measurement with the folin phenol reagent. J Biol Chem 193:265–275.

Ma P, Luo Q, Chen J, Gan Y, Du J, Ding S, et al. 2012. Intraperitoneal injection of magnetic $Fe_3O_4$-nanoparticle induces hepatic and renal tissue injury via oxidative stress in mice. Int J Nanomedicine 7: 4809–4818.

Moody AJ, Mitchell R, Jeal AE, Rich PR. 1997. Comparison of the ligand-binding properties of native and copper-less cytochromes bo from Escherichia coli. Biochem J 324:743–752.

OECD. 2008. Acute oral toxicity – up and down procedure. OECD test guideline 425 adopted 3rd October 2008. Paris: Organisation for Economic Cooperation and Development.

Paglia DE, Valentine WN. 1967. Studies on the quantitative and qualitative characterization of erythrocyte glutathione peroxidase. J Lab Clin Med 70:158–169.

Porter RK, Hulbert AJ, Brand MD. 1996. Allometry of mitochondrial proton leak: influence of membrane surface area and fatty acid composition. Am J Physiol 271:R1550–R1560.

Rømert P, Quistorff B, Bhenke O. 1993. Histological evaluation of the zonation of colloidal gold uptake by the rat liver. Tissue Cell 25:19–32.

Rouslin W, Millard RW. 1980. Canine myocardial ischemia: Defct in mitochondrial electron transfer complex I. J Mol Cell Cardiol 12: 639–645.

Sadauskas E, Wallin H, Stoltenberg M, Vogel U, Doering P, Larsen A, et al. 2007. Kupffer cells are central in the removal of nanoparticles from the organism. Part Fibre Toxicol 4:10.

Sammut IA, Thorniley MS, Simpkin S, Fuller BJ, Bates TE, Green CJ. 1998. Impairment of hepatic mitochondrial respiratory function following storage and orthotopic transplantation of rat livers. Cryobiology 36:49–60.

Scown TM, van Aerle R, Johnston BD, Cumberland S, Lead JR, Owen R, et al. 2009. High doses of intravenously administered titanium dioxidenanoparticles accumulate in the kidneys of rainbow trout but with no observableimpairment of renal function. Toxicol Sci 109: 372–380.

Sebekova K, Dusinska M, Simon Klenovics K, Kollarova R, Boor P, Kebis A, et al. 2014. Comprehensive assessment of nephrotoxicity of intravenously administered sodium-oleate-coated ultrasmall superparamagnetic iron oxide (USPIO) and titanium dioxide (TiO2) nanoparticles in rats. Nanotoxicology 8:142–57.

Schrand AM, Rahman MF, Hussain SM, Schlager JJ, Smith DA, Syed AF. 2010. Metal-based nanoparticles and their toxicity assessment. Wiley Interdiscip Rev Nanomed Nanobiotechnol 2(5):544–568.

Toblli JE, Cao G, Oliveri L, Angerosa M. 2011. Assessment of the extent of oxidative stress induced by intravenous ferumoxytol, ferric carboxymaltose, iron sucrose and iron dextran in a nonclinical model. Arzneimittelforschung 61(7):399–410.

Turrens J. 1997. Superoxide production by the mitochondrial respiratory chain. Biosci Rep 17:3–8.

Umbreit TH, Francke-Carroll S, Weaver JL, Miller TJ, Goering PL, Sadrieh N, et al. 2012. Tissue distribution and histopathological effects of titanium dioxide nanoparticles after intravenous or subcutaneous injection in mice. J Appl Toxicol 32:350–357.

van Ravenzwaay B, Landsiedel R, Fabian E, Burkhardt S, Strauss V, Ma-Hock L. 2009. Comparing fate and effects of three particles of different surface properties: Nano-$TiO_2$, pigmentary $TiO_2$ and quartz. Toxicol Lett 186:152–159.

Villalba JM, Navarro F, Cordoba F, Serrano A, Arrayo A, Crane FL, et al. 1995. Coenzyme Q reductase from liver plasma membrane: Purificationand role in trans-plasma-membrane electron transport. Proc Natl Acad Sci USA 92:4887–4891.

Wang J, Zhou G, Chen C, Yu H, Wang T, Ma Y, et al. 2007. Acute toxicity andbiodistribution of different sized titanium dioxide particles in mice after oral administration. Toxicol Lett 168:176–185.

Watts JA, Ford MD, Leonova E. 1999. Iron-mediated cardiotoxicity develops independently of extracellular hydroxyl radicals in isolated rat hearts. J Toxicol 37:19–28.

Weibel ER, Kistler GS, Scherle WF. 1966. Practical steriological methods formorphometric cytology. J Cell Biol 30:23–38.

Whittaker P, Hines FA, Robl MG, Dunkel VC. 1996. Histopathological evaluation of liver, pancreas, spleen, and heart from iron-overloaded Sprague-Dawley rats. Toxicol Path 24:558–563.

Wong SH, Knight JA, Hopfer SM, Zaharia O, Leach CN, Sunderman FW. 1987. Lipoperoxides in plasma as measured by liquid-chromatographic separation of malondialdehyde-thiobarbituric acid adduct. Clin Chem 33:214–220.